Including Aerosol Effects for Improved Visibility Forecasts in HARMONIE

Erik Marthinsen

Utrecht University and KNMI

August 2015

Supervisors

Sander Tijm (KNMI)

Aarnout van Delden (UU)

Koninklijk Nederlands Meteorologisch Instituut
Ministerie van Infrastructuur en Milieu

Universiteit Utrecht

Abstract

Today the numerical weather prediction model HARMONIE forecasts visibility based on the extinction coefficient of atmospheric hydrometeors (water droplets, ice crystals, graupel, etc.). Experience has shown that the visibility forecasts from HARMONIE are of poor quality, with HARMONIE forecasting either very low or very high visibility. The aim of this project is to improve the quality of the visibility forecasts by including the effect aerosols and the relative humidity have on visibility.

In the first part a set of diagnostic visibility functions are developed for visibility as a function of relative humidity and PM10 concentration. The functions are developed using observations of visibility, relative humidity, PM10 concentration and precipitation intensity at 13 weather stations in the Netherlands from the years 2012 and 2013. This diagnostic visibility function is intended to work alongside HARMONIE and be used in cases without precipitation, when aerosols are thought to be more important than hydrometeors in determining the visibility.

Further the quality of the forecasts from HARMONIE, the air chemistry model LOTOS-EUROS and the diagnostic visibility function is assessed using data from 2014. The diagnostic visibility function is used with both forecasts and observations of the input variables, in order to determine what impact the limitations in the forecasting of the input variables have on the quality of the visibility forecasts.

The results show that the visibility forecasts from the diagnostic visibility function have considerably higher quality than the visibility forecasts from HARMONIE. It is also found that limitations in the forecasting of the input variables act to significantly lower the quality of the forecasts from the diagnostic visibility function. When observations of the input variables are used, i.e. no forecasting errors in the input variables, the quality of the visibility forecasts from the visibility function is found to be comparable to the quality of the relative humidity forecasts from HARMONIE.

Contents

Chapter 1

Introduction

Visibility is one of the most intuitive characteristics of the atmosphere. It is simply a measure of how far away an object can be seen and recognized against its background. Historically visibility has been measured by human observers. Today, however, automated measurements with transmissometers and scatter meters are becoming more common, and in the Netherlands all visibility observations are now done by instruments. The visibility reflects the optical state of the atmosphere, and it is reduced by scattering and absorption of light along the path from the object to the observer. Under normal conditions the main factor reducing the visibility is scatter of light by atmospheric hydrometeors (water droplets, ice crystals, graupel, etc.) and aerosols.

Low visibility is of great concern for land, sea and air traffic. There are numerous documented cases where fog events (visibility $< 1000\,\mathrm{m}$) have lead to accidents, and according to Musk (1991) fog is the weather hazard drivers fear the most. Driving only becomes hazardous when the visibility is reduced to less than 200 m (Edwards, 1998), but air traffic is affected at higher visibility. At Schiphol airport the maximum number of planes that can take off and land is reduced when the visibility is less than 1500 m. When the visibility is low fewer runways are used and the distance between the planes is increased. High quality visibility forecasts are therefore not only important for improving safety by warning drivers/pilots of dangerous conditions, but also in economical terms by, for instance, reducing down-time and delays and increasing capacity for airports.

Forecasting visibility is a challenge for numerical weather prediction (NWP) models because visibility in a complex way depends on parameters like relative humidity, precipitation, vegetation, snow cover and aerosol concentration. In addition, fog events usually have small spatial and temporal scales, making it difficult to forecasts them correctly. The NWP model HARMONIE is one of the tools used by KNMI (Royal Dutch Meteorological Institute) for visibility forecasts in the Netherlands. Even this state-of-the-art model has problems with forecasting visibility, and experience shows that HARMONIE has a tendency to forecast either very low or very high visibility.

In HARMONIE the visibility is calculated based on the density of hydrometeors and empir-

ical relations between the density of the different hydrometeors and their extinction coefficients. Aerosol concentration and composition are not included as variables in HARMONIE, and so the effect of aerosols on visibility cannot be explicitly taken into account. The fact that aerosol effects are not included is thought to be a major reason for the poor quality of the visibility forecasts from HARMONIE.

The goal of this project is to improve the visibility forecasts from HARMONIE by taking account of the changing aerosol concentration and the effect this has on the visibility. To do this we will develop an empirical relation for visibility as a function of aerosol concentration and relative humidity (RH). This visibility function will be developed and used outside of precipitation events since we expect the visibility to be determined by the type and intensity of the precipitation, rather than the aerosol content of the air, in precipitation events. In the development of the visibility function observations from 2012 and 2013 of visibility, relative humidity, precipitation intensity and PM10 concentration at 13 weather stations in the Netherlands are used. With this function a new visibility variable is calculated using forecasts from 2014 of the precipitation intensity and relative humidity from HARMONIE and the PM10 concentration from the LOTOS-EUROS air chemistry model. The quality of the new visibility forecasts will be assessed by verification against observations (obs-verification).

The theory of visibility, the HARMONIE model and aerosols is presented in Chapter 2. In Chapter 3 the datasets used in this project and the statistical methods used to analyze the quality of forecasts are described. The empirical visibility function is also developed in this chapter. In Chapter 4 obs-verification is used to assess the quality of the forecasts from HARMONIE and LOTOS-EUROS. The quality of the new visibility variables calculated with the diagnostic visibility function is presented and discussed in Chapter 5. Finally, in Chapter 6 a brief summary is given before the main conclusions of the project are presented. A few suggestions for further work and implementation of the results from this project are also given in this last chapter.

Chapter 2

Theory

2.1 Visibility

When observing a distant object the apparent contrast between the object and its background decreases with increasing distance. This is a result of an increase in the apparent luminance of the object due to light being scattered into the observer's eyes by the air between the observer and the object, so-called airlight. At some distance the airlight will have increased the apparent luminance of the object to such a level that the apparent contrast between the object and its background becomes equal to the contrast threshold of the observer's eyes, and the object is barely visible. This distance is what is known as the visibility.

Based in this intuitive concept of visibility the World Meteorological Organization (WMO) has defined visibility as follows:

> Visibility, meteorological visibility (by day) and meteorological visibility at night are defined as the greatest distance at which a black object of suitable dimensions (located on the ground) can be seen and recognized when observed against the horizon sky during daylight or could be seen and recognized during the night if the general illumination were raised to the normal daylight level (WMO, 1992; 2003).

The visibility estimated by a human observer, based on the WMO definition, is affected by many subjective and physical factors. Primarily visibility is determined by the optical state of the atmosphere as represented by the atmospheric extinction coefficient. The extinction coefficient depends on the amount of particles (water droplets, aerosols etc.) in the atmosphere and their ability to scatter and absorb light. Scattering/absorption of light by these particles reduces the atmospheric visibility. The estimated visibility is also affected by the characteristics of the objects to be observed. In practice the objects used for observations in daylight may not be totally black, meaning they may have an intrinsic luminance. This

intrinsic luminance will reduce the contrast between the object and its background (the horizon sky), reducing the distance at which the objects can be seen. Hence, lighter colored objects are less visible than black objects and estimating visibility with such objects will underestimate the actual visibility of the atmosphere. In addition it is important to keep in mind that since the contrast threshold is subjective and varies from observer to observer visibility estimated by human observers will always be subjective. This means that two observers may have a different ability to recognize the object against its background, and may estimate a different visibility even when all outer factors are the same.

For consistency the measure of visibility to be used in meteorology should be objective and not influenced by any extra-meteorological factors. It must be a measure of the essential quantity, namely the transparency of the atmosphere, as well as being related to the intuitive concept of visibility as a measurement of how far away an object can be seen. To meet these requirements the meteorological optical range (MOR) has been defined and is now adopted by WMO as the measure of visibility. MOR is defined as the length of path in the atmosphere required to reduce the luminous flux in a collimated beam from a lamp burning at a color temperature of 2700 K (corresponding to a wavelength of about 550 nm) to 5 % of its original value (WMO, 2008).

2.1.1 Basic Equations

The primary equation when considering atmospheric visibility is the Bouguer-Lambert law:

$$F = F_0 e^{-\beta x} \tag{2.1}$$

where F is the luminous flux [lumen] received through an atmospheric length of path x from an object transmitting light with initial luminous flux F_0. The extinction coefficient β is defined as the proportion of luminous flux lost by a collimated beam (from a lamp burning at 2700 K) while traveling a unit distance in the atmosphere. The proportion of the luminous flux not lost by the beam while traveling from the object to the observer is called the transmission factor (T). Using equation 2.1 the transmission factor can be written as

$$T = \frac{F}{F_0} = e^{-\beta x} \tag{2.2}$$

From the definition of MOR it is clear that when an object is at MOR ($x = P$) the transmission factor is 0.05. Hence, for an object at MOR equation 2.2 gives

$$T = 0.05 = e^{-\beta P} \tag{2.3}$$

The mathematical relation between MOR and the extinction coefficient can then be written as

$$P = -\frac{\ln 0.05}{\beta} \approx \frac{3}{\beta} \tag{2.4}$$

showing that MOR only depends on the optical properties of the atmosphere.

By combining equations 2.2 and 2.4 the equation used for measuring MOR with a transmissometer (see subsection 2.1.2) can be obtained:

$$P = \frac{x \ln 0.05}{\ln T} \tag{2.5}$$

MOR is related to the intuitive concept of visibility through the contrast threshold (ε). The contrast threshold is the minimum value of the luminance contrast (C) that the human eye can detect. The luminance contrast is given by

$$C = \frac{L_b - L_h}{L_h} \tag{2.6}$$

where L_b is the luminance of the object $\left[\mathrm{cd\,m^{-2}}\right]$ and L_h is the luminance of the background. Note that the luminance contrast will be negative when the object is darker than the background. The relationship between the apparent contrast (C_x) between an object and its background when seen by an observer from a distance x, and the inherent contrast (C_0) the object would have against its background when seen from short range is given by Koschmieder's law:

$$C_x = C_0 e^{-\beta x} \tag{2.7}$$

From equation 2.6 the inherent contrast is $C_0 = -1$ when a black object ($L_b = 0$) is viewed against the background horizon, and from equation 2.7 the apparent contrast between the object and its background at a distance x is given by

$$C_x = -e^{-\beta x} \tag{2.8}$$

Comparing this result with equation 2.3 shows that when the apparent contrast is reduced to -0.05 the object is at MOR. Hence, MOR relates to the intuitive concept of visibility by being exactly the visibility that would be estimate by a human observer if the contrast threshold of the observer's eyes was 0.05.

2.1.2 Measuring Visibility

Historically visibility has been measured by human observers and this is still widely done. Each station has a list of objects suitable for both daytime observations (church towers, buildings, trees etc.) and night-time observations (light sources) at known distances and bearings from the station. The observations are made without any optical devices by observers who have "normal" vision and have received suitable training. Since the meteorological measuring stations in the Netherlands no longer use human observers to estimate visibility, the methods used by human observers will not be elaborated upon here, but details are provided in for instance WMO (2008).

Instruments used for estimating the visibility work by measuring the extinction coefficient from which MOR may be calculated using equation 2.4. From MOR the visibility may then be calculated based on the contrast threshold.

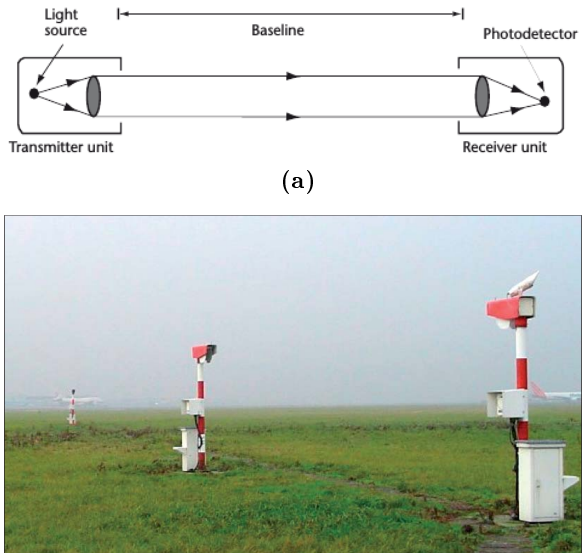

(a)

(b)

Figure 2.1: **(a)** Sketch of a transmissometer **(b)** Double baseline transmissometer located at Schiphol airport. Left in the picture are two receiver units at different distances from the transmitter unit seen to the right in the picture.
Source: (a) WMO (2008), (b) KNMI (2005)

Today all visibility measurements in the Netherlands are done by instruments, and in the measuring network of KNMI two kinds of instruments for measuring meteorological visibility are used: transmissometers and scatter meters.

Transmissometer: A transmissometer estimates MOR by determining the mean transmission factor of the atmosphere between a transmitter and a receiver. The transmitter sends a collimated light beam with known luminous flux (F_0) to the receiver where a photodetector measures the luminous flux transmitted through the atmosphere (F). From this the mean transmission factor can be calculated using equation 2.2. A simple sketch of a transmissometer is shown in Figure 2.1a.

The distance between the transmitter and the receiver is called the transmissometer baseline (a), and may range from a few meters to over 100 meters depending on the range of MOR values to be measured. The range of MOR values that can be measured for a given baseline is between about 1 and 25 times the baseline length. To extend the measuring range transmissometers with two receivers at different distances from the transmitter are sometimes used. At airports in the Netherlands such double baseline transmissometers are used with baselines of 12 m and 75 m. One example can be seen in Figure 2.1b.

With the known transmissometer baseline and the calculated transmission factor MOR estimated by the transmissometer can be calculated using equation 2.5:

$$P = \frac{a \ln 0.05}{\ln T} \tag{2.9}$$

Calculating MOR using this expression assumes that the transmission factor determined

Table 2.1: Technical specifications for the instruments used by KNMI to measure visibility

	Vaisala Mitras transmissometer	*Vaisala FD12P scatter meter*
Range	10 m - 3 km	10 m - 50 km
Resolution	1 m	1 m
Accuracy	10 % - 20 %	10 % for 10 m - 10 km, 20 % for 10 km - 50 km
Frequency	1/12 Hz	1/12 Hz

Source: KNMI (2005)

between the transmitter and the receiver is the same as that in the path between an observer and an object at MOR.

Since the transmissometer estimates MOR in a way that is so closely related to the definition of MOR, a transmissometer working within its range of highest accuracy provides a very good approximation to the true MOR (WMO, 2008).

Some technical specifications for the Vaisala Mitras transmissometer used in the KNMI measuring network are listed in Table 2.1.

Scatter meter: A scatter meter estimates MOR by measuring the scattering coefficient in a volume of air and assuming that the absorption coefficient in the atmosphere is negligible. In this way the extinction coefficient can be considered equal to this scattering coefficient. Since the visibility is mainly reduced by scattering of light on water droplets and aerosols, this assumption is usually good. The exception is if the air contains particles that strongly absorb light, e.g. industrial pollutants and ice crystals.

The scattering coefficient is determined by having a transmitter concentrate a beam of light on a small volume of air and using a photodetector to determine the proportion of the light scattered in a given angle. The most used technique measures the forward scatter and a sketch of such a scatter meter is shown in Figure 2.2a.

The scatter coefficient (β_{scat}) is given by the function

$$\beta_{scat} = \frac{2\pi}{\Phi_V} \int_0^{\pi} I(\phi) \sin(\phi)\, d\phi \tag{2.10}$$

where Φ_V is the flux entering the volume of air V and $I(\phi)$ is the intensity of the light scattered in direction ϕ with respect to the incident beam. In order to properly determine the scattering coefficient, measurements would have to be made of the light being scattered in all directions. In practice, however, the scattered light is only measured over a limited angle and the scattering coefficient is calculated assuming a high correlation between the intensity measured for the given angle and the full integral in equation 2.10. MOR can then be estimated from equation 2.4:

$$P = -\frac{\ln 0.05}{\beta_{scat}} \tag{2.11}$$

Since a scatter meter only samples a very small volume of air, the measured MOR is

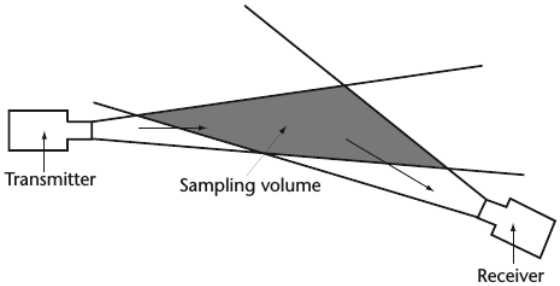

(a)

(b)

Figure 2.2: (a) Sketch of a scatter meter measuring forward scatter. **(b)** Scatter meter located in De Bilt
Source: (a) WMO (2008), (b) KNMI (2005)

usually less representative for the general state of the atmosphere than that measured by a transmissometer, which samples a larger volume.

Some technical specifications for the Vaisala FD12P scatter meter used in the KNMI measuring network is listed in Table 2.1, and a picture of the scatter meter located in De Bilt is shown in Figure 2.2b.

2.2 HARMONIE

HARMONIE is a mesoscale non-hydrostatic spectral model developed through collaboration between the HIRLAM consortium and the ALADIN consortium. The main objective of this cooperation is to provide the HIRLAM and ALADIN members with a state-of-the-art numerical weather prediction system for short range forecasting. HARMONIE is built upon model components that had previously been developed in the ALADIN and Météo-France communities, and at the default horizontal resolution of 2.5 km the forecast model is basically the same as the AROME model from Météo-France. At lower resolutions different physical packages and/or dynamical cores can be used.

At KNMI version 36h1.4 of HARMONIE is run operationally with a horizontal resolution of 2.5 km and 60 vertical levels. The boundary conditions for the operational model are provided by a larger scale HIRLAM 11 km model. The model is run every three hours with

a forecasting range of 48 hours and an output temporal resolution of one hour.

More information about HARMONIE can be found at the website of the HIRLAM consortium: www.hirlam.org.

2.2.1 Forecasting Visibility in HARMONIE

As seen from equation 2.4, MOR can be calculated once the extinction coefficient is known. The extinction coefficient can be calculated from theoretically derived relations if the extinction efficiency and size distribution of all the atmospheric constituents affecting visibility (hydrometeors, aerosols) are known. Since this is not known, except for in detailed field campaigns, empirically determined relations between the density of hydrometeors (W) and the extinction coefficient of each hydrometeor are used in practice.

In HARMONIE rain, snow, cloud droplets, ice crystals and graupel are prognostic variables and thus the scattering coefficient due to each of these hydrometeors can be calculated using the relations in Table 2.2. The total extinction coefficient of the atmosphere is then calculated as the sum of the hydrometeor's extinction coefficients plus a background extinction coefficient due to air molecules and the fixed background aerosol concentration:

$$\beta = \beta_{clw} + \beta_r + \beta_{ci} + \beta_s + \beta_g + \beta_b \tag{2.12}$$

$$\beta = 144.7W_{clw}^{0.88} + 1.1W_r^{0.75} + 163.9W_{ci}^{1.00} + 10.4W_s^{0.78} + 2.6W_g^{0.78} + \beta_b \tag{2.13}$$

The extinction due to an aerosol concentration different from the background concentration is not taken into account since aerosol concentration is not a prognostic variable in HARMONIE.

Given the expression for the extinction coefficient in equation 2.13 the visibility (MOR) is calculated with the relation

$$VIS = -\frac{\ln 0.02}{144.7W_{clw}^{0.88} + 1.1W_r^{0.75} + 163.9W_{ci}^{1.00} + 10.4W_s^{0.78} + 2.6W_g^{0.78} + \beta_b} \tag{2.14}$$

Note that the value 0.02 is used for the contrast threshold here, as opposed to 0.05 suggested by WMO (2008) and used in equation 2.4. The value 0.02 was suggested by Koschmeider (1924) and is widely used. When using 0.02 for the contrast threshold the calculated MOR will be about 30 % larger than when using a contrast threshold of 0.05.

2.3 Aerosols

Aerosols are defined as a suspension of fine solid or liquid particles in a gas (Seinfeld and Pandis, 2006). The particles are either released directly into the atmosphere (primary aerosols) or formed in the atmosphere by gas to particle conversion (secondary aerosols). Aerosols are emitted from both natural (sea salt, mineral dust, sulfates from DMS, etc.) and anthropogenic (industrial dust, fuel combustion, etc.) sources.

Table 2.2: Extinction coefficients for the different hydrometeors in HARMONIE. W is the density of the hydrometeor in $\mathrm{g\,m^{-3}}$.

Hydrometeor	*Extinction coefficient*
Cloud liquid water	$\beta_{clw} = 144.7W_{clw}^{0.88}$
Rain	$\beta_r = 1.1W_r^{0.75}$
Cloud ice	$\beta_{ci} = 163.9W_{ci}^{1.00}$
Snow	$\beta_s = 10.4W_s^{0.78}$
Graupel	$\beta_g = 2.6W_g^{0.78}$

Source: Petersen and Nielsen (2000)

The diameters of atmospheric aerosols range from a few nanometers to hundreds of micrometers, and based on the diameter the aerosols are classified as fine particles ($< 2.5\,\mu\mathrm{m}$) or coarse particles ($> 2.5\,\mu\mathrm{m}$). This division is fundamental since fine particles and coarse particles in general have different sources, sinks, chemical composition and optical properties. The fine aerosol mode can be further divided into two modes: the nucleation mode ($< 0.1\,\mu\mathrm{m}$) and the accumulation mode ($0.1 - 2.5\,\mu\mathrm{m}$). Aerosols in the nucleation mode are formed by condensation of gasses and are lost primarily by coagulation with larger particles. Aerosols in the accumulation mode are formed primarily when aerosols in the nucleation mode grow into this size range by coagulation and/or by condensation of water vapor. Aerosols in the accumulation mode are too big to grow efficiently by condensation, too few to grow efficiently by coagulation, and they are too small to be removed efficiently by dry deposition. This means that the aerosols in the accumulation mode are least efficiently removed from the atmosphere, hence the name of the mode. Aerosols in the coarse mode are formed by mechanical processes and consist of, for instance, natural and anthropogenic dust particles lifted by the wind. These aerosols have large enough sedimentation velocities to be removed by dry deposition.

In addition to the removal mechanisms described above, wet deposition affects both fine and coarse mode particles. Wet deposition causes the aerosols to be incorporated into cloud droplets during the formation of precipitation and/or be washed out of the atmosphere as the droplets fall. In combination these removal mechanisms lead to relatively short residence times for aerosols in the troposphere, typically days to a few weeks. Because of this short residence time and the spatial distribution of sources, aerosols vary in both concentration and composition over the Earth.

2.3.1 Aerosols and Visibility

The extinction of light by aerosols is a result of both scattering and absorption of the light, but for most aerosols scattering is by far the most important process. Each aerosol particle scatters and absorbs light with a certain efficiency know as the particle's scattering (σ_{scat}) and absorption (σ_{abs}) cross section, respectively. Depending on the optical properties of the aerosol particle and the wavelength of the incident light the scattering and absorption cross sections can be smaller or larger than the cross-sectional area of the particle (A). The ratio between the scattering cross section and the cross-sectional area of a particle is the

dimensionless scattering efficiency (Q_{scat}):

$$Q_{scat} = \frac{\sigma_{scat}}{A} \tag{2.15}$$

The absorption efficiency is similarly defined and the extinction efficiency of an aerosol particle is given by

$$Q_{ext} = Q_{scat} + Q_{abs} \tag{2.16}$$

By assuming that the atmospheric aerosols are spherical particles, equations for the scattering and absorption efficiency can be formally derived using Mie theory. The scattering and absorption efficiency are functions of the wavelength of the incident light (λ), the diameter of the aerosol particle (D_p) and the particle's complex index of refraction (m) giving the particle's optical properties relative to the surrounding atmosphere.

If the extinction efficiency and the size distribution of aerosols are known, in an atmosphere with a population of differently sized aerosols, the extinction coefficient due to the aerosols can be calculated using the following equation:

$$\beta_{aer} = \int_0^{D_p^{max}} \frac{\pi D_p^2}{4} Q_{ext}\left(\lambda, D_p, m\right) n\left(D_p\right)\, dD_p \tag{2.17}$$

where D_p^{max} is the diameter of the largest aerosol particle in the population, $n\left(D_p\right)$ is the number size distribution function and Q_{ext} is given by Mie theory.

The above discussion shows that four parameters determine the effect atmospheric aerosols have on visibility in an area. The complex reflective index and the diameter of the aerosol particles are necessary to calculate Q_{scat} and Q_{abs} which describe how effectively a single particle scatters and absorbs light. Then the aerosol number size distribution is needed to determine the extinction and absorption of light by the whole aerosol population. In addition the total number concentration of aerosols along the atmospheric path from the light source to the observer dictates how many scattering and absorption events the light beam will encounter.

Aerosol hygroscopicity and visibility: Some aerosols are hygroscopic meaning that they will attract and hold water molecules as the ambient relative humidity increases. This can have a huge effect on the visibility and is responsible for the situations with lowest visibility, namely fog.

The uptake of water changes the composition of the aerosols. If an aerosol is a liquid solution with some material dissolved in water the uptake of more water will dilute the aerosol. As the composition of the aerosol is changed, the refractive index is changed as well. This will in turn change the extinction efficiency of the aerosol. Since water has a smaller refractive index than most atmospheric aerosols, the uptake of water will generally decrease the refractive index of the aerosol, causing it to scatter less light. This effect will work to reduce the extinction efficiency of the aerosol.

The impact of aerosol dilution on visibility is small compared to the effect of the changing aerosol size (Tang, 1996). When the relative humidity increases hygroscopic aerosols will attract water vapor from the ambient air and start to grow. This growth starts at RH levels well below saturation. When the aerosols grow the total mass of the aerosols in a volume of air increases as well as the total surface area of the aerosols. For a single aerosol particle the scattering cross section will increase as it absorbs more water. The scattering cross section of an ammonium sulfate aerosol particle can, for example, increase by a factor five or more at 90 % RH compared to the dry particle (Malm and Day, 2001). This effect will work to greatly increase the scattering from aerosols as the relative humidity increases.

Not all aerosols are hygroscopic and different hygroscopic aerosols behave differently when the relative humidity increases. In order to determine the extinction of a light beam caused by aerosols it is therefore necessary to know which aerosol species are present as well as the relative humidity.

Chapter 3

Data and Methods

3.1 Datasets

3.1.1 Observations

In this project meteorological and air quality observations from 2012, 2013 and 2014 are used. The observations from 2012 and 2013 are used to develop a diagnostic visibility function. The observations from 2014 are used for obs-verification of the forecasts from HARMONIE and LOTOS-EUROS, and the visibility calculated using the diagnostic visibility function.

Meteorological observations: KNMI has 49 operational weather stations in the Netherlands, of which 13 are used in this project. The rejected stations either have a large amount of missing data or are considered to be poorly represented by the air quality measuring stations. The selected stations are shown on the map in Figure 3.1, and more information about the stations can be found in Table A.1.

In this project three meteorological variables are used: visibility [m], relative humidity [%] and precipitation intensity [mm/h]. The observations are reported as 10 minute averages, but in order to match the PM10 observations hourly averages are calculated and used for the analysis. The observations are reported in Coordinated Universal Time (UTC) and all the calculations are also performed in UTC.

PM10 observations: The PM10 concentration $[\mu g\, m^{-3}]$ is not measured at the weather stations in the KNMI network. It is rather measured at some of the stations in the Dutch National Air Quality Monitoring Network (LML) operated by the National Institute of Public Health and the Environment (RIVM). This network consist of 51 stations of which 16 are used in this project. The rejected stations do not measure PM10, have large amounts of missing data, or they are situated such that other stations better represent the conditions at the weather stations. The selected stations are shown on the map in Figure 3.1, and more information about the stations can be found in Table A.2.

Figure 3.1: Map of the selected observation stations in the Netherlands. Meteorological stations in red and air quality stations in blue

The PM10 observations are reported as hourly averages in local time, and are converted from local time to UTC prior to the calculations. Since the PM10 concentrations are measured in a different network than the meteorological variables, the position of the measuring stations are different. In the interest of having all the data available at the same positions, the PM10 observations are interpolated from the air quality stations to the weather stations. If an air quality station is located close to the weather station, the PM10 concentration at the weather station is taken to be equal to that measured at the air quality station. If the distance is larger, the PM10 observations from two or three air quality stations are interpolated to the weather station using inverse distance weighting.

3.1.2 Forecasts

In this project forecasts of meteorological variables and PM10 concentrations from 2014 are used. The meteorological forecasts are from HARMONIE, and the PM10 concentrations are from the LOTOS-EUROS model.

Meteorological forecasts: In the HARMONIE output files that were used the forecasts have already been interpolated from the regular grid of HARMONIE to the meteorological stations. Since HARMONIE is run every three hours with a forecasting range of 48 hours

there are many forecasts available for any given time. To have one continuous time series of the HARMONIE forecasts, only the 00 UTC runs are used with a forecasting range of 24 hours. Days are considered to start at 00 UTC. Each run will therefore give forecasts from 01 UTC the day of the run till 00 UTC the following day.

In the output files the precipitation intensity and visibility are reported as such, but the relative humidity must be calculated based on the forecasted 2 m temperature (T) and 2 m dewpoint temperature (T_d) using the relation

$$rh = 100\frac{e}{e_s} = 100\frac{e_s\left(T_d\right)}{e_s\left(T\right)} \tag{3.1}$$

where e and e_s are the vapor pressure and saturation vapor pressure, respectively. The saturation vapor pressure can, using the Magnus form approximation (Alduchov and Eskridge, 1996), be approximated by

$$e_s\left(T\right) = 6.1094\exp\left(\frac{17.625T}{243.04+T}\right) \tag{3.2}$$

Applying this approximation to equation 3.1 the relative humidity can be calculated using the relation

$$rh = 100\exp\left(\frac{17.625T_d}{T_d+243.04} - \frac{17.625T}{T+243.04}\right) \tag{3.3}$$

PM10 forecasts: The LOTOS-EUROS air chemistry model is an integration of the two models LOTOS (Long Term Ozone Simulation) and EUROS (European Operational Smog). The LOTOS model was developed by Netherlands Organization for Applied Scientific Research (TNO) and EUROS was developed by RIVM. One of the output variables from the LOTOS-EUROS model is PM10 concentration [kg/kg]. The operational LOTOS-EUROS model at KNMI has a horizontal resolution of 0.125° longitude × 0.0625° latitude, and from this grid the PM10 concentrations are interpolated to the weather stations. To convert the forecasted PM10 concentrations to the same unit as the observed concentrations they are multiplied with the density of air. In this project we take the density of air to be constant at $1.2\,\mathrm{kg\,m^{-3}}$. A simple calculation show that the extremes we might expect are about $1.13\,\mathrm{kg\,m^{-3}}$ (P=980 hPa; T=30 °C) and $1.38\,\mathrm{kg\,m^{-3}}$ (P=1040 hPa; T=−10 °C), and $1.2\,\mathrm{kg\,m^{-3}}$ therefore seems like a reasonable value to use for the air density.

3.2 Methodology

3.2.1 Development of a Diagnostic Visibility Function

In this project we intend to find an empirical relation between visibility, relative humidity and PM10 concentration. In the search for this relation we restrict ourselves to the cases without precipitation. This is because when there is precipitation we expect the visibility to be determined by the type and intensity of the precipitation, rather than the aerosol content

in the air, as the aerosols are washed out by the precipitation. Since HARMONIE includes hydrometeors as prognostic variables and presently calculates visibility based on their concentration (Section 2.2.1), we expect HARMONIE to be more accurate at forecasting visibility in precipitation and fog events than outside these events. Our empirical relation based on relative humidity and PM10 concentration will therefore act as an additional visibility relation to be used in cases without precipitation or fog, when we expect the aerosol effect to be the main factor reducing visibility.

Because poor visibility is a greater concern than good visibility we restrict our analysis to observations where the visibility is less than 20 km. Observations where one or more of the parameters are missing are not used. When we combine the 13 stations, apply these restrictions and remove the observations where there is precipitation, the number of observations amounts to 80 499.

In order to find the empirical relation, which is a plane in three dimensions, we first divide the observations into 20 bins, based on the PM10 concentration. The width of the bins are determined so each bin will have roughly the same number of observations, which in this case is around 4000. The width of the bins can be seen in Table 3.1.

Within each of the 20 bins we intend to find a relation between relative humidity and visibility. From these 20 relations the 3D plane can be constructed. In each bin the scatterplot of visibility vs. relative humidity shows a large amount of scatter, but it is also possible to see a clear pattern (Figure 3.2). In order to find the curve that will fit this pattern best, the median visibility within small bins of relative humidity are calculated. To make sure the fitting curve would catch the sharp decrease in visibility for relative humidity close to 100 %, the 10th percentiles are calculated in stead of the medians (50th percentile) for relative humidity close to 100 %. Else the scatter in observed values would draw the relations too far from the low visibilities. The medians are also plotted in Figure 3.2, and it can be seen that they "flatten out" in the lower relative humidity range. Orthogonal distance regression is used to make a linear fit to the medians at high relative humidity, before the medians flatten out. For some of the bins two linear fits have to be used: one for relative humidity below 97 %, and one above. The resulting curves (Table 3.1) are taken to be our empirical relations between visibility and relative humidity for each PM10 bin. It can be seen from Figure 3.2 that the linear fitting curves describe the observed patterns in the scatter plots well.

Using the forecasted relative humidity from HARMONIE and forecasted PM10 concentrations from LOTOS-EUROS a new visibility variable is made using the relations in Table 3.1. How well these new visibility forecasts compare to observations and the visibility forecasts from HARMONIE will be investigated in Chapter 5.

Table 3.1: Fitting curves for each PM10 bin

PM10 bin	*PM10 concentration* $[\mu g\,m^{-3}]$	*Fitting curve*
1	$0 - 7.3$	$-1817 \cdot rh + 180293$
2	$7.3 - 10.4$	$-1803 \cdot rh + 178984$
3	$10.4 - 12.7$	$-1717 \cdot rh + 170516$
4	$12.7 - 14.6$	$-1716 \cdot rh + 170275$
5	$14.6 - 16.2$	$-1684 \cdot rh + 167168$
6	$16.2 - 18.0$	$-1657 \cdot rh + 164467$
7	$18.0 - 19.6$	$-1566 \cdot rh + 155452$
8	$19.6 - 21.2$	$-1483 \cdot rh + 147339$
9	$21.2 - 22.8$	$-1290 \cdot rh + 128695$
10	$22.8 - 24.5$	$-1292 \cdot rh + 128594$
11	$24.5 - 26.3$	$-1200 \cdot rh + 119463$
12	$26.3 - 28.2$	$-1134 \cdot rh + 112929$
13	$28.2 - 30.3$	$-1069 \cdot rh + 106444$
14	$30.3 - 32.6$	$-851 \cdot rh + 86201$, for $rh < 97\,\%$ $-1703 \cdot rh + 168766$, for $rh \geq 97\,\%$
15	$32.6 - 35.5$	$-810 \cdot rh + 81747$, for $rh < 97\,\%$ $-1334 \cdot rh + 132545$, for $rh \geq 97\,\%$
16	$35.5 - 39.0$	$-702 \cdot rh + 71043$, for $rh < 97\,\%$ $-1358 \cdot rh + 134637$, for $rh \geq 97\,\%$
17	$39.0 - 43.7$	$-560 \cdot rh + 57162$, for $rh < 97\,\%$ $-1275 \cdot rh + 126501$, for $rh \geq 97\,\%$
18	$43.7 - 50.1$	$-487 \cdot rh + 49652$, for $rh < 97\,\%$ $-971 \cdot rh + 96620$, for $rh \geq 97\,\%$
19	$50.1 - 60.3$	$-344 \cdot rh + 35689$, for $rh < 97\,\%$ $-977 \cdot rh + 97108$, for $rh \geq 97\,\%$
20	$60.3+$	$-270 \cdot rh + 28021$, for $rh < 97\,\%$ $-749 \cdot rh + 74479$, for $rh \geq 97\,\%$

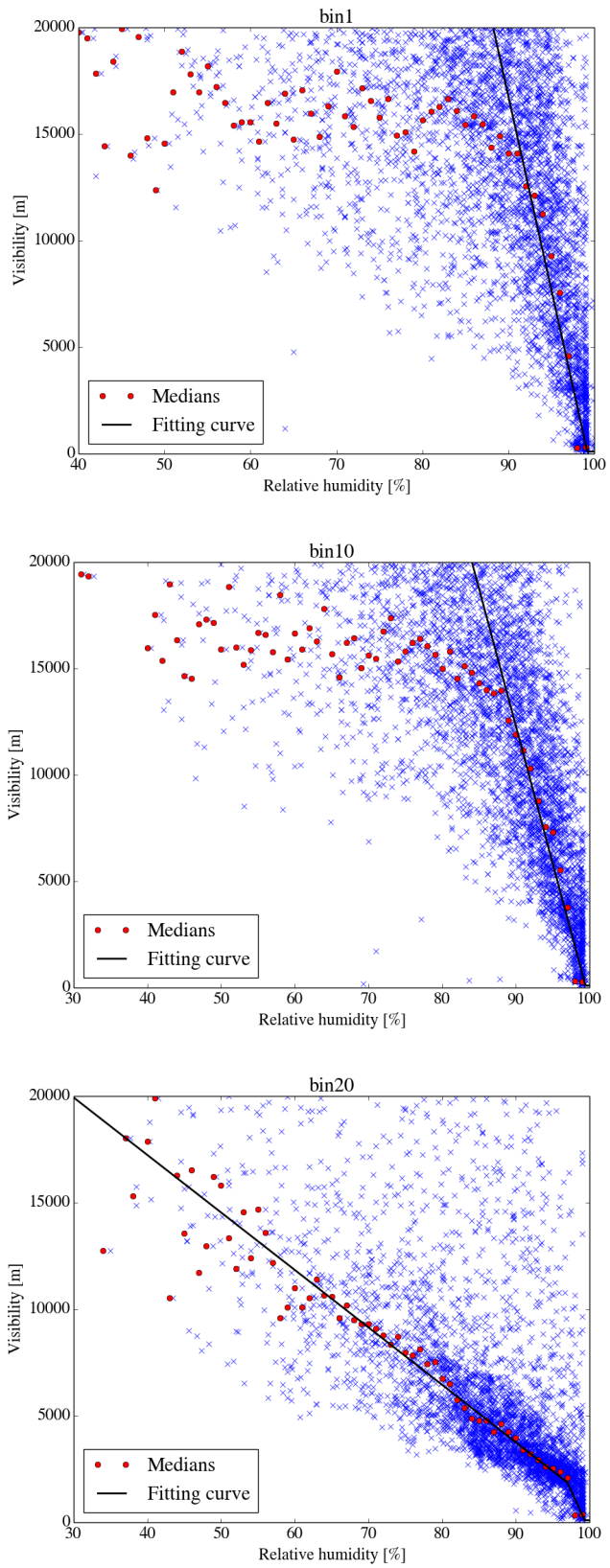

Figure 3.2: Scatterplots of visibility vs. relative humidity for some of the PM10 bins. The red circles indicate the median visibility in small bins of relative humidity. The black lines are the fitting curves from Table 3.1.

Table 3.2: Contingency table for evaluating forecasts

Forecasted	*Observed*	
	Yes	No
Yes	a	b
No	c	d

3.2.2 Statistical Methods

In this project the statistical methods suggested by Thornes and Stephenson (2001) are used to determine the quality of the forecasts. The quality is evaluated based on three attributes: reliability, accuracy and skill. To determine these attributes it is recognized that for any given event in forecasting a 2×2 contingency table, like the one in Table 3.2, can be made. The event can for instance be visibility less than 1000 m (fog). In Table 3.2 a is then the number of times fog is both forecasted and observed, b is the number of times fog is forecasted but not observed, c is the number of times fog is observed but not forecasted, and d is the number of times fog is neither forecasted nor observed. The forecasts are correct in a and d, while c is denoted as Type 1 error (miss) and b is denoted as Type 2 error (false alarm).

Reliability: The reliability of forecasts can be indicated by the bias (B). The bias will tell whether the forecasting model is consistently over- or under-forecasting the event. The bias can be calculated from the contingency table as

$$B = \frac{a+b}{a+c} \tag{3.4}$$

When the bias is larger than 1, often called positive bias, the model is over-forecasting the event and when the bias is smaller than 1 (negative bias) the model is under-forecasting the event. When $B = 1$ the forecasts are said to be perfectly reliable. Note that this does not mean that the forecasts are accurate.

In some cases a positive bias can be put into the model intentionally to guard against Type 1 errors. In the example with fog a positive bias would lower the number of unforecasted fog events and, since fog has a large impact on aviation and road traffic safety, this would be a "better safe than sorry" approach. The downside would be forecasting more fog events that never take place. This can have an economical cost when, for instance, air traffic is slowed down due to the forecasted fog.

Accuracy: The accuracy of forecasts can be indicated by two independent measures: the hit rate (H) and the false alarm rate (F).

The hit rate is the proportion of the observed events that were forecasted. In probability terms the hit rate is the probability that the event was forecasted given that it is observed,

$H = P\,(\text{forecasted}\,|\,\text{observed})$. From the contingency table the hit rate can be calculated as

$$H = \frac{a}{a+c} \tag{3.5}$$

The hit rate is a number between 0 and 1 where close to 1 indicates good accuracy. If there are no Type 1 errors the hit rate will be exactly 1. Note that the hit rate by itself can be misleading. In the fog example forecasting fog all the time would give a hit rate of 1, but the quality of the forecasts would still be very poor.

The false alarm rate is the proportion of the not observed events that were forecasted. In probability terms the false alarm rate is the probability that the event was forecasted given that it is not observed, $F = P\,(\text{forecasted}\,|\,\text{not observed})$. From the contingency table the false alarm rate can be calculated as

$$F = \frac{b}{b+d} \tag{3.6}$$

The false alarm rate is a number between 0 and 1 where close to 0 indicates good accuracy. If there are no Type 2 errors the false alarm rate will be exactly 0.

In the fog example forecasting fog all the time might give a hit rate of 1 (indicating very good accuracy), but it will also give a false alarm rate of 1 (indicating very poor accuracy). It is therefore important to look at both the hit rate and the false alarm rate in order to determine the accuracy of the forecasts.

Skill: The skill of the forecasts can be indicated by the Peirce skill score (PSS). PSS is simply calculated from the hit rate and the false alarm rate as

$$PSS = H - F \tag{3.7}$$

PSS is thus a measure of how good the forecasting model is at correctly forecasting the event and avoiding false alarms. The PSS is a number between -1 and 1 where the closer the value is to 1 the better the skill of the forecasts. If PSS is negative the false alarm rate is larger than the hit rate. The forecasting model would then have better skill if it simply relabeled forecasted events as unforecasted and vice versa.

In the fog example forecasting fog all the time would give a PSS of zero, indicating that the forecasting model has no skill.

Chapter 4

Quality of the Forecasts

In this chapter the quality of the forecasts from HARMONIE and LOTOS-EUROS is examined. The qualities of the forecasts are determined using the statistical methods described in Section 3.2.2. The quality of the visibility forecasts from HARMONIE will be used for comparison with the quality of the new visibility variable we have calculated using the diagnostic visibility function. This comparison will be done in Chapter 5. The quality of the forecasts of the other variables is also important. We use forecasted values of the meteorological and air quality variables in order to calculate the new visibility. The quality of our visibility calculations therefore depends on the quality of the forecasts of the variables we use.

4.1 HARMONIE

4.1.1 Precipitation Intensity

As explained in Chapter 3, the diagnostic visibility function will only be used when there is no precipitation. We are therefore interested in knowing only how good HARMONIE is at forecasting whether there will be precipitation or not, and not how well HARMONIE forecasts the intensity of the precipitation. In HARMONIE the amount of precipitation is often very small instead of exactly zero, and a threshold of 0.1 mm/h is therefore used for the forecasts in the obs-verification. If the forecasted precipitation intensity is lower than this, we consider there to be forecasted no precipitation and the visibility can be calculated using the visibility function. The obs-verification results in the simple 2×2 contingency table seen in Table 4.1 where the event is precipitation smaller than 0.1 mm/h.

Firstly, we see that no precipitation is observed in 91 % of the total number of cases, but no precipitation is forecasted in only 57 % of the cases. This gives a large negative bias of 0.63, and HARMONIE is clearly under-forecasting no precipitation.

The hit rate is high, telling us that as many as 61 % of the observed precipitation-free events were forecasted. The false alarm rate is low; when precipitation was observed HARMONIE

Table 4.1: Contingency table for precipitation intensity smaller than 0.1 mm/h. Total number: 111 650

Forecasted	*Observed*		*B*	*H*	*F*	*PSS*
	yes	no				
yes	61 942	2006	0.63	0.61	0.19	0.42
no	39 411	8291				

had forecasted there would be no precipitation in only 19 % of the cases. The combination of the hit rate and the false alarm rate results in a Peirce skill score of 0.42. This skill score is indicating that HARMONIE has good skill when it comes to forecasting whether there will be precipitation or not.

For our purpose it is most important that the false alarm rate is low in Table 4.1. In the obs-verification of the visibility forecasts from the diagnostic visibility function Type 2 errors in Table 4.1 will result in the calculated visibility being compared with the visibility observed during precipitation events. This will introduce an error in the obs-verification since the visibility is calculated assuming no precipitation. Type 1 errors, on the other hand, will result in the rejection of cases that should not have been rejected. This will lower the number of cases that can be used in the obs-verification and thus increase the statistical uncertainty, but it will not result in errors in the obs-verification. Hence, since the false alarm rate is low in the precipitation intensity forecasts from HARMONIE, using these forecasts when calculating the new visibility variable with the visibility function is expected to introduce few errors.

4.1.2 Relative Humidity

Unlike for the precipitation intensity we are interested in knowing the quality of the RH forecasts from HARMONIE for different values of RH. To accomplish this we have divided the RH range into five classes. The results of the obs-verification can therefore be presented in a 5×5 contingency table (Table 4.2). For each class the bias, hit rate, false alarm rate and Peirce skill score can be calculated by considering RH being in this class as the event. That is, for RH class 1 a from Table 3.2 is the number of cases where both the forecasted and observed RH is lower than 70 %, b is the number of cases where the forecasted RH is lower than 70 % but the observed RH is higher, c is the number of cases where the observed RH is lower than 70 % but the forecasted RH is higher, and d is the number of cases where both the forecasted and observed RH are higher than 70 %. For each class the 5×5 contingency table (Table 4.2) is thus reduced to a 2×2 contingency table, and the bias, hit rate, false alarm rate and PSS are calculated as normal. We can then evaluate the quality of the RH forecasts for the different classes.

The sum of the numbers on the main diagonal of the contingency table gives the number of correct forecasts, i.e. cases with the observed and forecasted relative humidity within the same class. The proportion of correct RH forecasts is 0.50. If we allow the forecasts to miss by one class the proportion, called the one class error, is 0.90. This means that in in 50 %

Table 4.2: Contingency table for relative humidity [%]. Total number: 111 268. Proportion of correct forecasts: 0.50. One class error: 0.90.

Forecasted	*Observed*					*B*	*H*	*F*	*PSS*
	< 70	$70-80$	$80-90$	$90-95$	$95-100$				
< 70	15 870	3570	1603	288	86	0.93	0.69	0.06	0.63
$70-80$	5448	8076	5688	1397	508	1.03	0.39	0.14	0.25
$80-90$	1569	7971	17 001	6432	3373	1.12	0.52	0.25	0.28
$90-95$	114	846	7042	7929	6351	1.19	0.42	0.16	0.27
$95-100$	11	77	1078	2738	6202	0.61	0.38	0.04	0.34

of the cases the forecasted RH was in the same class as the observed RH, and in 90 % of the cases the forecasted RH was at most one class different from the observed RH.

From Table 4.2 we see that the bias only deviate a little from 1 for the first four classes. For class 5 the bias is 0.61, meaning that HARMONIE is under-forecasting RH values in this class to such an extend that the number of times RH is forecasted to be in this class is only 61 % of the number of times it is observed to be in this class. From the relations for the diagnostic visibility functions we know that the visibility changes greatly with changes in RH, and especially in the RH-range covered by class 5. Since this range is associated with low visibility, the under-forecasting of RH in this range is expected to result in too few cases of low visibility in the new visibility variable calculated using the diagnostic visibility function.

The hit rates range from 0.38 for class 5 to 0.69 for class 1, indicating that the accuracy with which HARMONIE forecasts RH is quite good for all the classes.

The false alarm rates are low for all the classes, also indicating good accuracy for the RH forecasts. Especially class 1 and 5 have very low false alarm rates, reflecting the relatively small number of Type 2 errors for these classes.

For all the classes the combination of hit rate and false alarm rate results in a good PSS. For class 1 the PSS is over 0.60 and the other classes all have PSS over 0.25. This shows that HARMONIE definitely has skills when it comes to forecasting the relative humidity.

Table 4.3: Contingency table for visibility [km]. Total count: 22 752. Proportion of correct forecasts: 0.04. One class error: 0.12

Forecasted	*Observed*					*B*	*H*	*F*	*PSS*
	0 – 0.4	0.4 – 1	1 – 5	5 – 10	10 – 20				
0 – 0.4	551	590	6386	5780	5752	33.73	0.98	0.83	0.14
0.4 – 1	11	15	288	497	843	2.69	0.02	0.07	−0.05
1 – 5	0	4	178	396	823	0.20	0.03	0.08	−0.05
5 – 10	1	4	42	127	214	0.06	0.02	0.02	0.00
10 – 20	2	1	41	59	147	0.03	0.02	0.01	0.01

4.1.3 Visibility

The proportion of correct visibility forecasts from HARMONIE is low. In only 4 % of the cases did HARMONIE forecast the visibility to be in the same class as the observed visibility. By allowing the forecasts to miss by one class this percentage still only increases to 12 %, meaning that in as many as 88 % of the cases the visibility forecasts from HARMONIE miss by two classes or more.

The bias is huge for class 1. Dense fog (visibility < 400 m) is forecasted by HARMONIE more than 33 times as often as it is observed. Also class 2 has a large bias. The combination of class 1 and 2 gives how often fog is forecasted/observed, and it is clear from Table 4.3 that HARMONIE greatly over-forecasts fog. The biases of the remaining classes are necessarily strongly negative since these classes must be vastly under-forecasted when class 1 and 2 are so vastly over-forecasted. This extreme distribution of the forecasted visibility from HARMONIE can be seen clearly in the scatterplot in Figure 4.1. The scatterplot shows a strong tendency for the forecasted visibility to be lower than the observed visibility. In particular HARMONIE' leaning towards forecasting dense fog can be clearly seen.

HARMONIE forecasted dense fog in more than 83 % of the total number of cases, but it was only observed in 2 % of the cases. For class 1 this results in very few Type 1 errors, and consequently a high hit rate. For the other classes the hit rates are very low, reflecting the large number of times visibility is observed to be in these classes, but forecasted to be in class 1.

The strong over-forecasting of dense fog also results in a high false alarm rate for class 1. For the other classes the false alarm rates are very low. This is a result of the relatively few Type 2 errors occurring for these classes when the visibility is forecasted to be in class 1 almost every time.

The PSS are very low for all classes, except class 1, indicating that HARMONIE has very poor skills at forecasting visibility in these classes. For class 1 the visibility forecasts have some skill. Based on Table 4.3 it must therefore be said that HARMONIE has poor skills when it comes to forecasting visibility.

We see that the quality of the visibility forecasts from HARMONIE stands out by being far

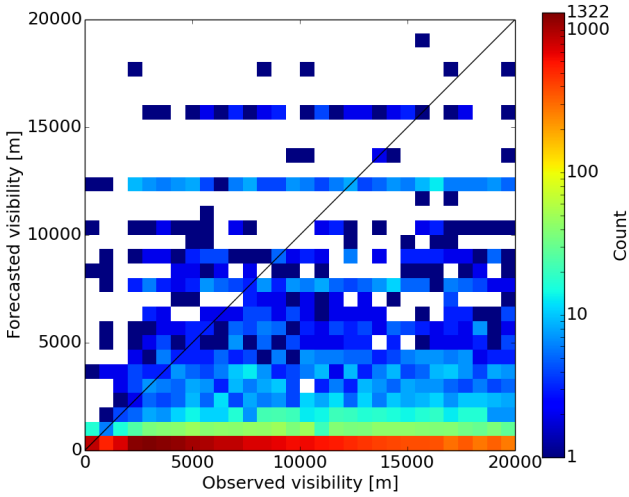

Figure 4.1: Scatterplot of HARMONIE forecasted visibility vs. observed visibility. The color indicates the number of cases with forecasted and observed visibility within that double bin. The black diagonal line indicates where the forecasted and observed visibility are equal.

poorer than the quality of the other forecasts. This comes as no surprise since this whole project was initiated based on the knowledge that HARMONIE was forecasting visibility poorly. In Chapter 5 we will examine if the quality of the visibility calculated using the diagnostic visibility function is any better.

4.2 LOTOS-EUROS

4.2.1 PM10

Ideally the quality assessment of the PM10 forecasts would use classes equal to the PM10 bins used in Section 3.2.1. This is however very unpractical since it would call for a 20×20 contingency table. To be consistent with the obs-verification of RH and visibility from above, we instead present the results in a 5×5 contingency table (Table 4.4). The classes are defined such that each class covers four of the PM10 bins from Section 3.2.1.

From Table 4.4 we see that in 37 % of the cases the forecasted PM10 concentration from LOTOS-EUROS is within the same class as the observed PM10 concentration, and in 76 % of the cases the forecasted concentration was at most one class different from the observed concentration.

There is a positive bias for PM10 concentrations in class 1 and 2, indicating that these classes with low PM10 concentration are being over-forecasted by LOTOS-EUROS. PM10 concentrations in class 3, 4 and 5 are under-forecasted by LOTOS-EUROS. Especially PM10 concentrations in class 5 are strongly under-forecasted. It is clear from Table 4.4 that the PM10 concentrations are generally forecasted to be too low by LOTOS-EUROS. For observations in class 2 LOTOS-EUROS forecasts more cases with PM10 in class 1 than in

Table 4.4: Contingency table for PM10 concentration $[\mu g\, m^{-3}]$. Total number: 93 792. Proportion of correct forecasts: 0.37. One class error: 0.76

Forecasted	*Observed*					B	H	F	PSS
	0 - 14.6	14.6 - 21.2	21.2 - 28.2	28.2 - 39	39+				
0 - 14.6	18 884	10 544	5206	2463	827	1.19	0.59	0.31	0.28
14.6 - 21.2	8235	7538	4953	3182	1540	1.08	0.32	0.25	0.07
21.2 - 28.2	3100	3504	3272	3111	2077	0.95	0.21	0.15	0.05
28.2 - 39	1384	1534	1875	2477	3223	0.86	0.20	0.10	0.10
39+	364	407	563	964	2565	0.48	0.25	0.03	0.22

class 2, and the number of cases in class 1 is much higher than the number of cases in class 3, 4 and 5. For observations in class 3 LOTOS-EUROS forecasts more cases in both class 1 and class 2 than in class 3, and the number of cases forecasted in class 4 and 5 are much lower. Similarly, for observations in class 4 the forecasts have more cases with PM10 concentrations in both class 2 and class 3 than in class 4. Since high PM10 concentrations are associated with low visibility for all values of RH (Table 3.1), the tendency of LOTOS-EUROS to forecast too low PM10 concentrations is expected to cause the visibility function to forecasts too high visibility when the forecasted PM10 concentrations are used as input.

The hit rates vary from 0.20 for class 4 to 0.59 for class 1. The false alarm rate is very low for class 5 as a result of the relatively few cases where the PM10 concentration is forecasted to be in this class. For the other classes the false alarm rates range from 0.10 for class 4 to 0.31 for class 1.

The PSS are low for class 2, 3 and 4, meaning that LOTOS-EUROS has poor skills when it comes to forecasting PM10 concentrations in these classes. For class 1 and 5 the PSS are better.

The forecasts of PM10 concentration appear to have a lower quality than the forecasts from HARMONIE, with the exception of visibility. The true error in the forecasts of PM10 may come from the LOTOS-EUROS model itself forecasting too low PM10 concentrations. Note that some of the reduction in quality might also have been introduced by our methods. The observed PM10 concentrations are not considered at the location where they are measured, but are rather interpolated to the weather stations. The observations of PM10 might be made under conditions that are not representative for the weather station, e.g. close to a road or in a city, which would result in too high PM10 concentrations at the weather station. The forecasted PM10 concentrations are also interpolated from a regular grid to the weather stations, and this interpolation might cause errors. Also, in order to get the forecasted PM10 concentrations to have the same unit as the observed concentration, namely $[\mu g\, m^{-3}]$, we multiplied them with the density of air. Since this density is taken to be constant in this project we introduce an additional error, as discussed in Section 3.1.2.

Chapter 5

Results and Discussions

In this chapter the quality of the visibility forecasts from the diagnostic visibility function developed in Section 3.2.1 is assessed. The visibility function calculates the visibility using forecasted values of precipitation intensity and relative humidity from HARMONIE, and PM10 concentrations from LOTOS-EUROS. The forecasts of these input variables are themselves not perfect, as discussed in Chapter 4. The deviation of the input variables from the observations will affect the quality of the visibility forecasts. In order to determine the true quality of the visibility function itself, without the effect of the errors in the input variables, the visibility is also calculated using observations of the variables. The errors associated with the observations themselves and the interpolation of the PM10 values will still remain.

It is also of interest to see how the forecasts of the different input variables affect the quality of the visibility forecasts. This is investigated in Section 5.3 by using the visibility function with observations of one input variable, and forecasts of the other two.

Lastly, the quality of the visibility forecasts from a combination of the visibility function and HARMONIE is assessed in Section 5.4. In this case the visibility is calculated using the visibility function as long as there is forecasted no precipitation, and the visibility is calculated from the combined extinction coefficient from HARMONIE and the visibility function when there is forecasted precipitation.

Table 5.1: Contingency table for calculated visibility [km]. Only forecasts. Total number: 21 561. Proportion of correct forecasts: 0.45. One class error: 0.86.

Forecasted	*Observed*					*B*	*H*	*F*	*PSS*
	$0-0.4$	$0.4-1$	$1-5$	$5-10$	$10-20$				
$0-0.4$	214	139	609	196	57	2.19	0.39	0.05	0.34
$0.4-1$	53	38	244	76	23	0.73	0.06	0.02	0.04
$1-5$	182	226	1801	960	323	0.58	0.30	0.11	0.19
$5-10$	66	119	2163	2733	1716	0.94	0.38	0.28	0.09
$10-20$	40	76	1245	3303	4959	1.36	0.70	0.32	0.38

5.1 Only Forecasts

In this section the quality of the forecasts from the visibility function is assessed when only forecasts of the input variables are used. This will be a measure of how well the visibility function might perform in an operational setting where only forecasts are available.

5.1.1 Quality

The contingency table for the obs-verification of the visibility that is forecasted using forecasts of all the input variables is shown in Table 5.1. The information in this contingency table is also shown in Figure 5.2 where the quality assessment attributes of all the different scenarios presented in this chapter is summarized for easy side by side comparison.

For the visibility forecasted using the diagnostic visibility function the percentage of correct forecasts is 45 %, and when allowing the forecasts to miss by one class the percentage increases to 86 %.

There is a positive bias of 2.19 for class 1, indicating that the visibility function is forecasting dense fog more than twice as often as it is observed. The function has a negative bias for forecasting visibility in class 2, and by combining class 1 and 2 the bias of the function for forecasting fog is found to be 1.43. Hence, the visibility function is over-forecasting fog. The bias for class 4 is close to one, whereas the function is under-forecasting visibility in class 3, and over-forecasting visibility in class 5.

The hit rate is highest for class 5 where 70 % of the observed cases were forecasted. For class 2 the hit rate is lowest, and for this class as little as 6 % of the observed cases were forecasted. For the remaining classes the hit rates vary from 0.30 to 0.39.

For class 1 the false alarm rate is an order of magnitude lower than the hit rate. In only 5 % of the cases where the visibility was observed to be in another class was it forecasted to be in class 1. For class 2 the false alarm rate is even lower. For the remaining classes the false alarm rates are higher, ranging from 0.11 for class 3 to 0.32 for class 5. The low false alarm rates show that the visibility forecasts have relatively few Type 2 errors, which is a sign of good accuracy.

The combination of the hit rate and the false alarm rate gives the PSS of the visibility function. From Table 5.1 it can be seen that the function has good skills when it comes to forecasting visibility in class 1 and 5, with a PSS of 0.34 and 0.38, respectively. For class 2 and 4 the PSS are considerably lower, only 0.04 for class 2 and 0.09 for class 4. These PSS are significantly different from zero ($P < 0.01$), meaning that the visibility function has skills when it comes to forecasting visibility in these classes, although these skills are poor. For class 3 the PSS is 0.19.

5.1.2 Discussion

The percentage of correct forecasts from the diagnostic visibility function is considerably higher than that from HARMONIE (Section 4.1.3). In 88 % of the cases the visibility forecasts from HARMONIE will miss by two classes or more, whereas the forecasts from the visibility function will miss by that much in only 14 % of the cases. The visibility function is forecasting the right visibility class ten times as often as HARMONIE, and the one class error says that when the visibility function misses it is likely to miss by less than HARMONIE.

The bias for forecasting fog, and especially dense fog, was huge in HARMONIE. By combining class 1 and 2 in the HARMONIE forecasts it is found that fog was forecasted 17.19 times more often than it was observed. The visibility function also over-forecasts fog, but only by a factor 1.43, which must be considered to be a large improvement. As a result of the less extreme bias for fog the visibility function also show less extreme biases for the remaining classes, which HARMONIE was vastly under-forecasting. The biases in the visibility forecasts in Table 5.1 have, except for class 1, magnitudes within the same range as the magnitudes of the biases in the RH forecasts from HARMONIE and the PM10 forecasts from LOTOS-EUROS. The bias for class 1 in the visibility function is, however, larger than the biases seen for the other variables.

The positive bias for forecasting dense fog in the visibility function comes from the way the fitting curves are found in Section 3.2.1. The fitting curves describe the overall pattern in how the visibility changes with RH within each PM10 bin. This overall pattern shows a clear decrease in visibility with increasing RH, with dense fog for the highest values of RH (Figure 3.2). The diagnostic function will therefore forecast dense fog every time the RH is above a certain limit, and this limit is different for the different PM10 bins. The linear fits cannot describe the scatter in the observations around this general trend. It can be seen in Figure 3.2 that the scatter in the visibility observations are considerable, and for very high values of RH the visibility observations span the entire visibility range, even though most of the visibility observations indicate low visibility. Not accounting for this scatter, but rather forecasting dense fog every time the RH is above a certain limit, the visibility function will forecast more dense fog than is observed, and thus give a positive bias.

Also interesting is the negative bias for visibility in class 2. In HARMONIE this class had a large positive bias, albeit not as extreme as class 1. The scatter in the observations is probably limiting the visibility function's ability to correctly forecast visibility in class 2.

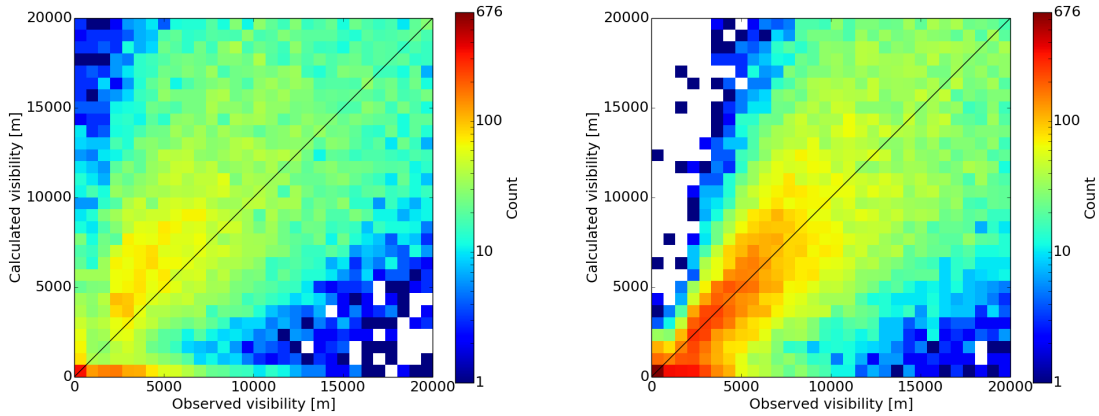

(a) **(b)**

Figure 5.1: Scatterplots of calculated vs. observed visibility. The color represents the number of cases with forecasted and observed visibility within that double bin. The black diagonal line indicates where the calculated and observed visibility are equal. **(a)** Visibility calculated with only forecasts of the input variables. **(b)** Visibility calculated with only observations of the input variables.

However, this is not the main cause of the negative bias for class 2 in the visibility function. As will be discussed in Section 5.2 and 5.3 this is rather caused by the limitations in the forecasts of the input variables.

For visibility forecasts in class 1 HARMONIE showed an almost perfect hit rate. This was, however, mainly because HARMONIE forecasted dense fog in almost all cases. The false alarm rate was therefore also high, resulting in a PSS of only 0.14. For the visibility function the hit rate for class 1 has decreased. This would in itself indicate that the accuracy is poorer than in HARMONIE, but in the forecasts from the visibility function the false alarm rate is one order of magnitude lower than in the HARMONIE forecasts, resulting in a PSS for class 1 that is much higher than in HARMONIE. For all other classes HARMONIE had a very low hit rate due to the large number of times visibility was observed to be in these classes, but forecasted to be in class 1. The visibility function shows a similarly low hit rate only for class 2. The low hit rate for class 2 is also a result of the limitations in the forecasts of the input variables (Section 5.2 and 5.3). For the remaining classes the hit rates are one order of magnitude higher than in HARMONIE. The false alarm rates are also higher than in HARMONIE, but compared to the hit rates they are relatively lower, resulting in higher PSS for the visibility function than for HARMONIE in all classes. Hence, the visibility function has better skills than HARMONIE for forecasting the visibility in all classes.

From Table 5.1 it can be seen that the forecasted visibility is generally too high. When the visibility is observed to be in class 2 the visibility function forecasts the visibility to be in every other class more often than in class 2, and the number of cases where the visibility is forecasted to be in class 3 is higher than the number of cases where it is forecasted to be in class 1 and 2 combined. For observed visibility in class 3 the visibility function forecasts more cases with visibility in class 4 than in class 3, and the number of cases with forecasted visibility in class 4 and 5 is remarkably higher than the number of cases with forecasted

Table 5.2: Contingency table for calculated visibility [km]. Only observations. Total number: 32 439. Proportion of correct forecasts: 0.56. One class error: 0.93.

Forecasted	*Observed*					*B*	*H*	*F*	*PSS*
	$0-0.4$	$0.4-1$	$1-5$	$5-10$	$10-20$				
$0-0.4$	232	266	683	120	30	2.38	0.41	0.03	0.38
$0.4-1$	197	249	1029	188	44	2.42	0.35	0.05	0.31
$1-5$	131	187	4898	2456	841	1.04	0.60	0.15	0.45
$5-10$	0	2	1440	5041	3247	0.87	0.45	0.22	0.23
$10-20$	0	1	174	3367	7616	0.95	0.65	0.17	0.48

visibility in class 1 and 2. Similarly, for observed visibility in class 4 the visibility function forecasts more cases with visibility in class 5 than in class 4, and the number of cases with forecasted visibility in the other classes is much lower. This tendency of the visibility function to forecast too high visibility can be seen even clearer in the scatterplot in Figure 5.1a. Apart from the over-forecasting of the very low visibility we see that the general trend is that the forecasted visibility is higher than the observed visibility. The tendency of the visibility function to forecast too high visibility might be a result of the tendency of LOTOS-EUROS to forecast too low PM10 concentrations, as suggested in Section 4.2.1. This will be investigated further in the following sections.

When comparing the scatterplot in Figure 5.1a with the scatterplot for HARMONIE in Figure 4.1, it again becomes clear that the forecasts from the visibility function are in much better agreement with the observations than the visibility forecasts from HARMONIE.

5.2 Only Observations

In this section the quality of the forecasts from the visibility function is assessed when only observations of the input variables are used. This is of course not possible in an operational setting, but it will provide insight into how well the visibility function performs in itself, regardless of the quality of the forecasts of the other variables. This can be considered as an upper limit for the performance of the visibility function in the operational setting. If the forecasting models were forecasting the input variables perfectly the visibility function would still have limitations. It wouldn't forecast the visibility perfectly, but rather with the quality found in this section.

5.2.1 Quality

The contingency table for the obs-verification of the visibility that is forecasted using observations of all the input variables is shown in Table 5.2. The information in this contingency table is also shown in Figure 5.2 where the quality assessment attributes of all the different scenarios presented in this chapter is summarized for easy side by side comparison.

When using observations of the input variables the visibility function has a percentage of correct forecasts of 56 %. When allowing the forecasts to miss by one class the percentage increases to 93 %. This means that if the input variables were in perfect agreement with the observations the visibility forecasts from the diagnostic function would miss by more than one class in only 7 % of the cases.

There are strong positive biases for class 1 and 2, and by combining the two classes the bias of the function for forecasting fog is found to be 2.40. Hence, the visibility function is clearly over-forecasting fog when observations of the input variables are used. For the remaining classes the biases are close to one.

The hit rates are high for all classes, ranging from 0.35 for class 2 to 0.65 for class 5. This in combination with low false alarm rates results in high PSS, ranging from 0.23 for class 4 to 0.48 for class 5.

5.2.2 Discussion

The differences in quality between forecasts in this section and the forecasts from Section 5.1 are caused by the limitations in in the forecasts of the input variables used by the visibility function. There is also a difference in the total number of cases making up Table 5.2 and Table 5.1, but since the number is high in both the statistical uncertainty is low in both cases.

Compared to the results with only forecasts the percentage of correct forecasts and one class error have increased considerably when only observations are used. The one class error is remarkably high, indicating that if the input variables to the visibility function were in perfect agreement with the observations the visibility function would only miss by more than one class in 7 % of the cases.

The biases are also different between the two cases. Especially noticeable is the increase in bias for class 2. This class changes from having a negative bias of 0.73 in the case with only forecasts to a strong positive bias of 2.42 in the case with only observation. It is therefore clear that the limitations in the forecasts of one or more of the input variables are causing the negative bias for class 2 seen in the case with only forecasts, since the visibility function itself is over-forecasting visibility in class 2. This will be discussed further in Section 5.3 where the effects of the forecasts of each variable are investigated.

The increase in the bias for class 2 combined with a small increase in the bias for class 1 results in a bias for forecasting fog that is higher in the observational case than in the forecasting case. Hence, the visibility function itself if biased towards forecasting fog and will forecast fog more than twice as often as it is observed. For class 3 and 5 the observational case have a bias closer to one than the forecasting case, indicating that limitations in the forecasts of the input variables are causing the visibility forecasts to have larger biases for these classes.

For class 1 there is only a slight increase in the hit rate and a slight decrease in the false alarm rate when observations of the input variables are used. This causes the PSS for class

1 to increase by only 0.04. Hence, for class 1 going from forecasts to observations of the input variables will only have a small effect on the hit rate, false alarm rate and skill. The quality of the visibility forecasts for class 1 from the visibility function therefore seems to not be limited by the forecasts of the input variables, but rather by the visibility function itself.

For class 2, 3 and 4 the hit rates are considerably higher when observations of the input variables are used. The false alarm rates for class 2 and 3 increases slightly, whereas the false alarm rate for class 4 is decreasing. As a result the PSS for these classes increase significantly when going from forecasts to observations of the input variables. Hence, the quality of the visibility forecasts for class 2, 3 and 4 are limited by the forecasts of the input variables as well as the visibility function itself.

The PSS is lowest for class 4, and this is less than 0.30 even when observations of the input variables are used. This shows that the visibility function has considerable limitations when it comes to forecasting visibility in this class. This is due to the large amount of scatter in the visibility observations around the range covered by class 4, scatter which a linear fitting curve for visibility as a function of RH cannot account for.

For class 5 the hit rate is lower when observations of the input variables are used. This is mostly due to the fact that this class is forecasted less often in the observational case, which is indicated by the reduced bias. This reduction in hit rate for class 5 is, however, more than made up for by a considerable decrease in the false alarm rate, resulting in a PSS that is much higher when observations of the input variables are used. The quality of the visibility forecasts for class 5 is therefore also limited by the forecasts of the input variables as well as the visibility function itself.

From Table 5.2 it can be seen that the tendency for the calculated visibility to be higher than the observed visibility is reduced when only observations are used. Both for observations in class 3 and 4 the same class have the highest occurrences in the forecasts now. For both of these classes it is still the case that there are more forecasts in the class above than in the class below, but the difference is much lower than when forecasts of the input variables are used. When the observed visibility is in class 1 the visibility function never forecasts the visibility to be more than 5 km, and when the observed visibility is in class 2 this only happens 3 times. Hence, the number of cases where the visibility function forecasts the visibility to be much higher than the observed visibility is now reduced to almost zero. Also from the scatterplots in Figure 5.1 we see that the distribution seems to be more symmetrical and centered on the diagonal line in the observational than in the forecasting case. This goes to show that most of the visibility function's tendency to forecast too high visibility is caused by the limitations in the forecasts of the input variables.

5.3 Some Observations

In this section the quality of the forecasts from the visibility function is assessed when observations of one of the input variables are used. This will provide insight into how the limitations of the forecasts of the different input variables affect the quality of the forecasts from the visibility function. The contingency tables for the obs-verification of the visibility that is forecasted using observations of some of the input variables are shown in Table 5.3. The information in these contingency tables is also shown in Figure 5.2 where the quality assessment attributes of all the different scenarios presented in this chapter is summarized for easy side by side comparison.

5.3.1 Quality

Observed precipitation intensity: When observations of the precipitation intensity are used the visibility function has a percentage of correct forecasts of 0.46. When allowing the forecasts to miss by one class the percentage increases to 87 %.

The forecasts have a strong positive bias for class 1, and a negative bias for class 2. By combining class 1 and 2 the bias of the function for forecasting fog is found to be 1.41. For class 4 the bias is exactly one, so visibility in this class is forecasted as often as it is observed. The visibility function is under-forecasting visibility in class 3, and over-forecasting visibility in class 5.

For class 2 the hit rate is very low, and in this class only 6 % of the observed cases were forecasted. The hit rates for the other classes are higher, ranging from 0.30 for class 3 to 0.69 for class 5. For class 1, 2 and 3 the false alarm rates are very low, which results in good PSS for class 1 and 3. Class 2 has a low PSS due to the low hit rate. For class 4 the false alarm rate is high compared to the hit rate, resulting in a PSS of only 0.09. Class 5 has the highest false alarm rate, but it also has the highest hit rate resulting in class 5 having the highest PSS.

Observed relative humidity: When observations of the relative humidity are used the visibility function has a percentage of correct forecasts of 0.51. When allowing the forecasts to miss by one class the percentage increases to 91 %.

The forecasts have a strong positive bias for class 1 and 2, and by combining the two classes the bias of the function for forecasting fog is found to be 2.16. Hence, the visibility function is clearly over-forecasting fog when observations of RH are used. The function is under-forecasting visibility in class 3 and 4, and over-forecasting visibility in class 5, albeit not as strongly as it is over-forecasting visibility in class 1 and 2.

The hit rates are high for all the classes, ranging from 0.35 for class 2 to 0.68 for class 5. For class 4 the false alarm rate is so high compared to the hit rate that the PSS is 0.16. For the remaining classes the combinations of hit rates and false alarm rates result in high PSS, ranging from 0.30 to 0.44.

Observed PM10 concentration: When observations of the PM10 concentrations are used the visibility function has a percentage of correct forecasts of 50 %. When allowing the forecasts to miss by one class the percentage increases to 89 %.

The forecasts have a strong positive bias for class 1. The bias for visibility in class 2 is negative, and by combining class 1 and 2 the bias of the function for forecasting fog is found to be 1.54. Hence, the visibility function is over-forecasting fog when observations of PM10 concentrations are used. The function is under-forecasting visibility in class 3 and 4, albeit the bias for class 4 is quite close to one. Visibility in class 5 is over-forecasted by the visibility function.

For class 2 the hit rate is low, with only 7 % of the observed cases being forecasted. For the remaining classes the hit rates are high, ranging from 0.40 for class 3 to 0.69 for class 5. The false alarm rates for class 1 and 2 are of order 1%, which results in a high PSS for class 1. For class 2, however, the low hit rate causes the PSS to be low. For the remaining classes the false alarm rates are an order of magnitude larger, but they are still quite low. The PSS for these classes range from 0.14 for class 4 to 0.43 for class 5.

5.3.2 Discussion

Using the observations of precipitation intensity has a small impact on the quality of the forecasts from the visibility function. This comes as no surprise since the precipitation intensity is not used in itself when calculating the visibility. It is only used to determine in which cases the visibility should be calculated using the visibility function. The quality of the precipitation intensity forecasts would only affect the quality of the visibility forecasts if there were many cases where HARMONIE forecasted no precipitation, but precipitation was observed. In these cases the visibility would be calculated with the visibility function assuming no precipitation, but the forecasts would be compared to observations where there is precipitation. From Table 4.1 it is clear that this only happens in a few cases since HARMONIE is over-forecasting precipitation. The precipitation intensity might, however, have an impact on the quality of the forecasts when the visibility function is combined with the visibility forecasts from HARMONIE (Section 5.4). In this model the forecasted precipitation intensity from HARMONIE determines when the visibility is calculated with the visibility function alone, and when it is calculated from a combination of the visibility function and HARMONIE. The over-forecasting of precipitation in HARMONIE will then result in the combination of HARMONIE and the visibility function being used too often.

The proportion of correct forecasts and the one class error show the greatest increase when observations of RH are used, but the increase when using PM10 observations are only 0.01 and 0.02 lower, respectively. Since the proportion of correct forecasts and one class error is larger in the observational case than when either RH observations or PM10 observations are used alone, the combination of the two variables is important. Hence, the forecasts of both RH and PM10 are important for the difference in the proportion of correct forecasts and one class error between the forecasting and observational case, and only a combination

Table 5.3: Contingency tables for calculated visibility [km]. Some observations.

(a) Observed precipitation intensity. Total number: 31 958. Proportion of correct forecasts: 0.46. One class error: 0.87.

Forecasted	*Observed*					*B*	*H*	*F*	*PSS*
	$0-0.4$	$0.4-1$	$1-5$	$5-10$	$10-20$				
$0-0.4$	203	150	709	228	68	2.25	0.36	0.04	0.32
$0.4-1$	47	40	284	94	28	0.67	0.06	0.02	0.04
$1-5$	175	272	2442	1339	476	0.58	0.30	0.10	0.20
$5-10$	87	172	2912	3766	2666	1.00	0.39	0.30	0.09
$10-20$	48	115	1682	4171	7124	1.27	0.69	0.32	0.37

(b) Observed relative humidity. Total number: 23 302. Proportion of correct forecasts: 0.51. One class error: 0.91.

Forecasted	*Observed*					*B*	*H*	*F*	*PSS*
	$0-0.4$	$0.4-1$	$1-5$	$5-10$	$10-20$				
$0-0.4$	268	231	543	103	31	2.10	0.48	0.04	0.44
$0.4-1$	181	216	791	160	22	2.23	0.35	0.05	0.30
$1-5$	112	163	3001	1464	542	0.84	0.47	0.13	0.34
$5-10$	0	3	1480	3096	1858	0.80	0.38	0.22	0.16
$10-20$	0	2	510	3268	5257	1.17	0.68	0.24	0.44

(c) Observed PM10 concentration. Total number: 20 684. Proportion of correct forecasts: 0.50. One class error: 0.89.

Forecasted	*Observed*					*B*	*H*	*F*	*PSS*
	$0-0.4$	$0.4-1$	$1-5$	$5-10$	$10-20$				
$0-0.4$	200	129	571	186	42	2.42	0.43	0.05	0.38
$0.4-1$	39	36	211	66	19	0.74	0.07	0.02	0.05
$1-5$	143	198	2208	1215	311	0.74	0.40	0.12	0.28
$5-10$	56	94	1770	3050	1727	0.91	0.41	0.27	0.14
$10-20$	29	47	754	2833	4750	1.23	0.69	0.26	0.43

of the two can explain the full magnitude of the difference.

For class 1 it was noted in Section 5.2 that the difference between the forecasting and the observational case is small. It is therefore interesting to see in Table 5.3 that if only observations of RH are used the quality of the visibility forecasts in class 1 improves considerably. For all classes knowing RH will cause improved visibility forecasts for the same reason. For each PM10 bin the visibility function is a function of only RH. Knowing the real value of RH means that the difference in the calculated visibility and the observed visibility is caused by the scatter in the observed visibility for this given RH value. Since this scatter depends on which PM10 bin we are in the scatter is reduced from 3D (RH, PM10, visibility) to 2D (PM10, visibility), and the chance that the calculated visibility is close to the observed visibility is higher. The increased quality when the observations of RH are used seems to be counteracted by a reduction in quality when the observations of precipitation intensity are used. This causes the quality to only increase slightly when observations of all input variables are used.

For class 2 it can be seen that using the observations of PM10 concentration or precipitation intensity only has a minimal effect on the bias and hit rate. Hence, the large difference in the quality of the visibility forecasts in class 2 between the forecasting and observational case is explained exclusively by the quality of the RH forecasts from HARMONIE. Since the visibility range covered by class 2 is small compared to the slope of the fitting curves in the visibility function, only a very small range of RH values is associated with visibility in class 2. The RH forecasts from HARMONIE are not perfect and they will easily fall outside this narrow range, causing HARMONIE to forecast either too low or too high visibility compared to the observation. Knowing the values of RH will, as explained above, reduce the amount of possible scatter.

For class 3 there is an improvement in the bias, hit rate and PSS when either RH observations or PM10 observations are used. The improvement when all observations are used is, however, larger than either one. Hence, the quality of the RH forecasts from HARMONIE and the PM10 forecasts from LOTOS-EUROS are both affecting the quality of the visibility function for class 3, and the combined effect is larger than the effect of either one alone.

For class 4 and 5 a combination of the variables is also causing the difference between the forecasting case and the observational case. For these classes it is not possible to conclude that the quality of the forecasts of either RH or PM10 have the greatest influence on the quality of the forecasts from the visibility function.

It can be seen from Table 5.3 that the tendency of the visibility function to forecast too high visibility is reduced when observations of either RH or PM10 concentration are used. Hence, the tendency we found for LOTOS-EUROS to forecast too low PM10 concentrations is not causing all the difference in the over-forecasting of too high visibility between the observational and forecasting case. The limitations in the RH forecasts from HARMONIE are also important.

5.4 Combination Model

In this section the quality of the forecasts from a combination of the visibility function and the visibility forecasts from HARMONIE is assessed. As long as HARMONIE forecasts there will be no precipitation the visibility is calculated using the diagnostic visibility function. When HARMONIE forecasts that there will be precipitation the visibility is calculated using the equation

$$VIS_{comb} = -\frac{\ln(0.02)}{\beta_{calc} + \beta_{HARM}} \tag{5.1}$$

where the extinction coefficients β_{calc} and β_{HARM} are calculated from the visibility forecasted by the visibility function and HARMONIE, respectively. To simulate the operational setting only forecasts of the input variables are used in this section.

5.4.1 Quality

The contingency table for the obs-verification of the visibility that is forecasted using the combination of the visibility function and the visibility forecasts from HARMONIE is shown in Table 5.4. The information in this contingency table is also shown in Figure 5.2 where the quality assessment attributes of all the different scenarios presented in this chapter is summarized for easy side by side comparison.

When the visibility forecasted with the diagnostic function is combined with the visibility forecasted by HARMONIE the percentage of correct forecasts is 34 %. When allowing the forecasts to miss by one class the percentage increases to 65 %.

The forecasts have a huge positive bias for class 1, and the visibility is forecasted to be in class 1 almost 15 times as often as it is observed to be in this class. The combination model is therefore greatly over-forecasting dense fog. Visibility in class 2 is also over-forecasted, and by combining class 1 and 2 the bias of the combination model for forecasting fog is found to be 9.48. For class 5 the bias is exactly 1, whereas the combination model is under-forecasting visibility in class 3 and 4.

The hit rate for class 2 is very low, with only 5 % of the observed cases being forecasted. For the other classes the hit rates are an order of magnitude larger, ranging from 0.20 for class 3 to 0.53 for class 5. For most of the classes the false alarm rates are large compared to the hit rates, resulting in only class 5 having a PSS larger than 0.20. For class 2 and 4 the PSS are of order 0.01, indicating that the combination model has low skills when it comes to forecasting visibility in these classes.

5.4.2 Discussion

The visibility calculated using the combination of HARMONIE forecasted visibility and the visibility function shows a quality that is somewhere between the two models.

Table 5.4: Contingency table for calculated visibility [km]. Combination model. Total number: 36 094. Proportion of correct forecasts: 0.34. One class error: 0.65.

Forecasted	*Observed*					*B*	*H*	*F*	*PSS*
	$0-0.4$	$0.4-1$	$1-5$	$5-10$	$10-20$				
$0-0.4$	283	262	3327	3064	2832	14.96	0.43	0.27	0.17
$0.4-1$	57	43	366	310	294	1.35	0.05	0.03	0.03
$1-5$	184	234	1949	1192	637	0.43	0.20	0.09	0.11
$5-10$	75	144	2543	3256	2257	0.69	0.27	0.21	0.06
$10-20$	54	111	1638	4222	6760	1.00	0.53	0.26	0.27

The proportion of correct forecasts and one class error are considerably larger than for HARMONIE alone. The proportion of correct forecasts is now almost as large as for the PM10 forecasts from LOTOS-EUROS, but the one class error is somewhat lower.

The bias for class 1 is still large in the combination model, but it is only half the value of the bias in HARMONIE. For the remaining classes the biases are much better than for HARMONIE alone, and they are not more extreme than the biases found for the other variables. From Table 4.3 it was clear that HARMONIE barely forecasts visibility in the range $1-20$ km. That is no longer the case in the combination model (Table 5.4).

For class 1 the hit rate is lower in the combination model as a result of the combination model not forecasting dense fog as often as HARMONIE. The false alarm rate has also greatly decreased, but it is much higher than in the visibility function using only forecasts of the input variables. The false alarms therefore mainly come from the situations where HARMONIE has forecasted precipitation and subsequently very low visibility. It is clear that HARMONIE will usually forecast a too large extinction coefficient when it forecasts precipitation. Since the combination model uses a simple addition of the extinction coefficients from HARMONIE and the visibility function, the fact that HARMONIE is prone to over-estimate the visibility reduction in precipitation cases cannot be improved by using the combination model. The visibility forecasts from HARMONIE will therefore cause the combination model to over-forecast dense fog, resulting in a large false alarm rate compared to the visibility function alone. The PSS for class 1 in the combination model is slightly higher than in HARMONIE.

As previously discussed the visibility function is struggling with forecasting visibility in class 2 correctly due to the quality of the RH forecasts from HARMONIE. The visibility forecasts from HARMONIE also show a low quality when it comes to forecast visibility in class 2. It therefore comes as no surprise that the combination model shows a low quality for forecasting visibility in class 2. The hit rate and false alarm rate are slightly better than in HARMONIE alone, resulting in a PSS that is now positive. The PSS is, however, very small, indicating that the combination model also has poor skills when it comes to forecasting visibility in class 2.

For class 3, 4 and 5 the hit rates are considerably higher in the combination model than in HARMONIE. For class 3 the false alarm rate has only increased slightly, resulting in a PSS that is 0.16 higher than in HARMONIE. For class 4 and 5 the false alarm rates have increased more. For class 4 this results in a very low PSS, whereas for class 5 the increase

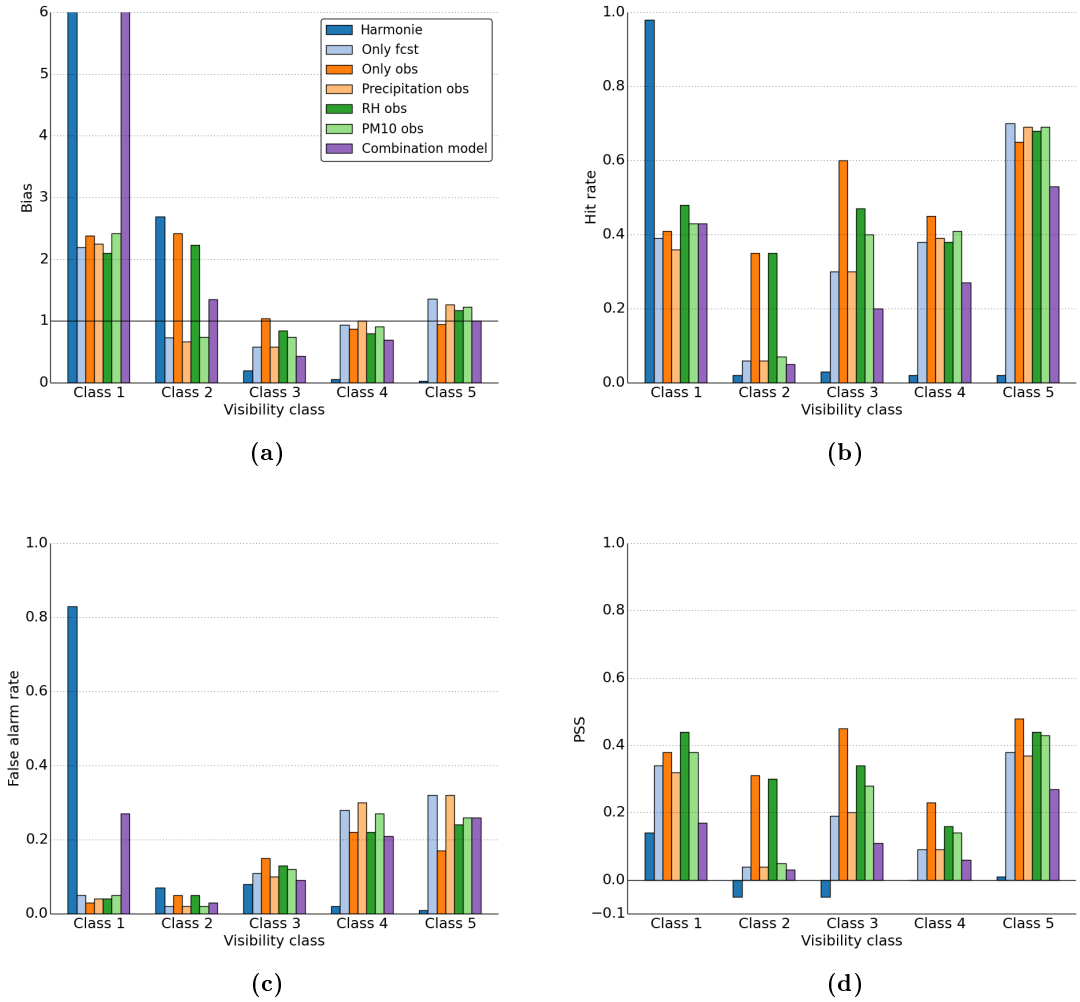

Figure 5.2: Quality assessment attributes for the different models and scenarios. **(a)** Reliability/bias. **(b)** Accuracy/hit rate. Legend is the same as in (a). **(c)** Accuracy/false alarm rate. Legend is the same as in (a). **(d)** Skill/Peirce skill score. Legend is the same as in (a).

in false alarm rate is relatively small compared to the increase in hit rate, resulting in the highest PSS of all the classes.

The combination model has better skills than HARMONIE for all classes. The skills of the combination model for forecasting visibility is of comparable size to the skills of the LOTOS-EUROS model for forecasting PM10 concentration (Table 4.4). The skills of HARMONIE for forecasting the relative humidity are higher.

Chapter 6

Summary and Conclusions

Summary: In this project we intended to improve the visibility forecasts from HARMONIE by taking the effect aerosols have on visibility into account. Our approach to this complex problem was to use observations of relative humidity, precipitation intensity, PM10 concentration and visibility to develop a diagnostic visibility function to be used for forecasting visibility when there is no precipitation. The idea behind this approach was that when there is no precipitation the visibility will mainly be determined by the aerosol content of the air and, through aerosol hygroscopicity, the relative humidity.

After the diagnostic visibility function was developed the quality of the forecasts of precipitation intensity, relative humidity and visibility from HARMONIE, and the forecasts of PM10 concentration from LOTOS-EUROS was assessed. The quality of the forecasts was determined by verifying the forecasts from 2014 against observations. This analysis provided us with a reference point with which to compare the performance of the diagnostic visibility function. Since these forecasts are used as input variables to the visibility function the quality of the forecasts also gave important insight into where the limitations in the forecasts from the visibility function might come from. We saw that the quality of the forecasts were generally good, except for the visibility forecasts from HARMONIE. This, however, came as no surprise since this whole project was initiated based on knowledge that HARMONIE is lacking when it comes to forecasting visibility.

In Chapter 5 the results of the calculations using the diagnostic visibility function were presented. The function was used to forecast the visibility in a few different scenarios. We simulated an operational setting by using forecasts of all the input variables. Calculations were also done using observations of one or all the input variables in order to determine how the forecasts of the different input variables affect the quality of the visibility forecasts. Lastly we combined the visibility function with the forecasted visibility from HARMONIE to calculate the visibility also in precipitation events.

Conclusions: Based on the results presented in Chapter 4 and 5 some conclusions can be drawn.

The visibility forecasts from the diagnostic visibility function have higher quality than the visibility forecasts from HARMONIE. The distribution of the forecasts have greatly improved and the skills for forecasting the visibility have increased for all the visibility classes we used for the quality assessment. When forecasts of the input variables are used the quality of the visibility forecasts from the visibility function are higher than the quality of the forecasts of PM10 concentration from LOTOS-EUROS. The quality is, however, lower than the quality of the RH forecasts from HARMONIE.

Some of the reduction in quality in the forecasts from the visibility function are caused by limitations in the forecasts of the input variables. For all classes the forecasts from the visibility function have higher skills when observations of the input variables are used than when forecasts are used. When observations of the input variables are used the quality of the visibility forecasts from the visibility function is comparable to the quality of the RH forecasts from HARMONIE.

The impact of using observations instead of forecasts of precipitation intensity had only a minimal effect on the quality of the forecasted visibility. However, this result must be treated with caution as the true effect of the over-forecasting of precipitation by HARMONIE is likely to be seen only when the forecasts from the visibility function is combined with the visibility forecasts from HARMONIE.

Using observations of either RH or PM10 concentration increases the quality of the visibility forecasts significantly compared to the case with only forecasts. Hence, limitations in the forecasts of RH from HARMONIE and PM10 concentration from LOTOS-EUROS both reduce the quality of the visibility forecasts from the visibility function.

The combination model forecasts visibility with higher quality than HARMONIE alone. The proportion of correct forecasts and one class error have increased considerably. The skills are also better for all visibility classes. The skills of the combination model is of comparable size to the skills of LOTOS-EUROS for forecasting the PM10 concentration. The combination model is vastly over-forecasting dense fog, even though the bias is only half the value of the bias in HARMONIE.

Future work and implementation: This project can only be considered a first approach to including the effect of aerosols in the visibility forecasts from HARMONIE. The promising results encourage further investigation into this topic.

Before the results of this project might be implemented in operational work it would be beneficial to combine the 20 individual visibility functions into one function. This would result in in a visibility function of the form $vis = f\left(RH, PM10\right)$ describing the 3D surface. If the diagnostic visibility function is to be implemented in operational work it is also important to examine the quality of the visibility forecasts for weather stations other than the ones used here to develop the function.

The PM10 forecasts from the LOTOS-EUROS model are reported on a different grid than the forecasts from HARMONIE. An interpolation of the PM10 concentrations to the same grid is therefore necessary before the visibility function can be used operationally.

Appendix A

Measuring Stations

Table A.1: Weather stations used in this project. AWS = Automatic Weather Station, A = Aerodrome.

Station number	*Name*	*Type*	*Latitude [N]*	*Longitude [E]*
6210	Valkenburg	AWS	52.17	4.42
6240	Schiphol	A/AWS	52.30	4.77
6269	Lelystad	A/AWS	52.45	5.53
6275	Deelen	A/AWS	52.07	5.88
6279	Hoogeveen	A/AWS	52.73	6.52
6280	Groningen	A/AWS	53.13	6.58
6319	Westdorpe	AWS	51.23	3.83
6340	Woensdrecht	A/AWS	51.45	4.33
6344	Rotterdam	A/AWS	51.95	4.45
6350	Gilze Rijen	A/AWS	51.57	4.93
6375	Volkel	A/AWS	51.65	5.70
6377	Ell	AWS	51.20	5.77
6380	Maastricht	A/AWS	50.92	5.78

Table A.2: Air quality measuring stations used in this project. The stations are classified based on location: R = Rural, UB = Urban Background, S = Street.

Station number	*Name*	*Type*	*Latitude [N]*	*Longitude [E]*
131	Vredepeel - Vredeweg	R	51.54	5.85
133	Wijnandsrade - Opfergeltstraat	R	50.90	5.88
235	Huijbergen - Vennekenstraat	R	51.43	4.36
236	Eindhoven - Genovevalaan	S	51.47	5.47
240	Breda - Tilburgseweg	S	51.59	4.82
318	Philippine - Stelleweg	R	51.29	3.75
404	Den Haag - Rebecquestraat	UB	52.08	4.29
448	Rotterdam - Bentinckplein	S	51.93	4.46
537	Haarlem - Amsterdamsevaart	S	52.38	4.65
631	Biddinghuizen - Hoekwantweg	R	52.45	5.62
633	Zegveld - Oude Meije	R	52.14	4.84
738	Wekerom - Riemterdijk	R	52.11	5.71
741	Nijmegen - Graafseweg	S	51.84	5.86
818	Barsbeek - De Veenen	R	52.65	6.02
929	Valthermond - Noorderdiep	R	52.88	6.93
937	Groningen - Europaweg	S	53.22	6.58

References

Alduchov, O. A. and R. E. Eskridge (1996, April). Improved magnus form approximation of saturation vapor pressure. *J. Appl. Meteor. 35*(4), 601–609.

Clark, P. A., S. A. Harcourt, B. Macpherson, C. T. Mathison, S. Cusack, and M. Naylor (2008, Oct). Prediction of visibility and aerosol within the operational met office unified model. i: Model formulation and variational assimilation. *Quarterly Journal of the Royal Meteorological Society 134*(636), 1801–1816.

Edwards, J. B. (1998, Dec). The relationship between road accident severity and recorded weather. *Journal of Safety Research 29*(4), 249–262.

KNMI (2005). *Handboek Waarnemingen*. KNMI.

Koschmieder, H. (1924). Therie der horizontalen sichtweite. *Beitr. Phys. Freien Atmosph* (12), 33 – 53 171 – 181.

Kunkel, B. A. (1984, January). Parameterization of droplet terminal velocity and extinction coefficient in fog models. *J. Climate Appl. Meteor. 23*(1), 34–41.

Malm, W. C. and D. E. Day (2001, June). Estimates of aerosol species scattering characteristics as a function of relative humidity. *Atmospheric Environment 35*(16), 2845–2860.

Musk, L. (1991). Climate as a factor in the planning and design of new roads and motorways. *Highway meteorology*, 1–25.

Petersen, C. and N. W. Nielsen (2000). *Diagnosis of visibility in DMI-HIRLAM*. Danish Meteorological Institute.

Seinfeld, J. and S. N. Pandis (2006). *Atmospheric chemistry and physics: from air pollution to climate change* (2nd ed.). John Wiley & Sons, Inc., Hoboken, New Jersey.

Tang, I. N. (1996). Chemical and size effects of hygroscopic aerosols on light scattering coefficients. *Journal of Geophysical Research 101*(D14), 19245.

Thornes, J. E. and D. B. Stephenson (2001, Sep). How to judge the quality and value of weather forecast products. *Meteorological Applications 8*(3), 307–314.

World Meteorological Organization (1992). International meteorological vocabulary. *WMO-NO. 182*.

World Meteorological Organization (2003). Manual on the global observing system. *WMO-NO. 544*.

World Meteorological Organization (2008). Guide to meteorological instruments and methods of observation. *WMO-NO. 8*.